Degradation of all-inkjet-printed organic thin-film transistors with TIPS-pentacene under processes applied in textile manufacturing

H. F. Castro [a], E. Sowade [b], J. G. Rocha [a], P. Alpuim [c], A.V. Machado [d],

R. R. Baumann [b], S. Lanceros-Méndez [c,*]

[a] Algoritmi Research Center, University of Minho, 4800-058 Guimarães, Portugal

[b] Digital Printing and Imaging Technologies, Chemnitz University of Technology, 09107 Chemnitz, Germany

[c] Department/Center of Physics, University of Minho, 4710 - 057 Braga, Portugal

[d] IPC/Departamento de Engenharia de Polímeros, Universidade do Minho, 4800-058 Guimarães, Portugal

[*] Corresponding author: Tel. +351 253 604 073, fax: +351 253 678 981, e-mail address: lanceros@fisica.uminho.pt.

Abstract

Printed electronics represent an alternative solution for the manufacturing of low-temperature and large area flexible electronics. The use of inkjet printing is showing major advantages when compared to other established printing technologies such as, gravure, screen or offset printing, allowing the reduction of manufacturing costs due to its efficient material usage and the direct-writing approach without requirement of any masks. However, several technological restrictions for printed electronics can hinder its application potential, e.g. the device stability under atmospheric or even more stringent conditions. Here, we study the influence of specific mechanical, chemical, and temperature treatments usually appearing in manufacturing processes for textiles on the electrical performance of all-inkjet-printed

organic thin-film transistors (OTFTs). Therefore, OTFTs where manufactured with silver electrodes, a UV curable dielectric, and 6,13-bis(triisopropylsilylethynyl) pentance (TIPS-pentacene) as the active semiconductor layer. All the layers were deposited using inkjet printing. After electrical characterization of the printed OTFTs, a simple encapsulation method was applied followed by the degradation study allowing a comparison of the electrical performance of treated and not treated OTFTs. Industrial calendering, dyeing, washing and stentering were selected as typical textile processes and treatment methods for the printed OTFTs. It is shown that the all-inkjet-printed OTFTs fabricated in this work are functional after their submission to the textiles processes but with degradation in the electrical performance, exhibiting higher degradation in the OTFTs with shorter channel lengths (L=10 μm).

Keywords: Organic thin-film transistors, printed electronics, inkjet-printing, organic electronic degradation.

1. Introduction

Organic electronics (OE) has the potential to become a market of large value over the next decades, mainly based on the use of sensors and active devices such as OTFTs, considering their critical role as electrical switches, amplifiers or memory elements. The reduced cost per area and the scalability to large-area is intrinsic to printing technologies and allows mass production for item level applications, without a significant cost surplus [1]. Furthermore, the use of printed electronics based on solution-processable materials provides a technical advantage since different functional materials can be deposited in ambient conditions in an additive manufacturing manner. In particular, the use of inkjet printing for printed electronics is increasingly gaining interest [2]–[4] due to the advantages of non-contact, high precision and maskless additive patterning, print layout flexibility and low material waste.

Textiles are a demanding but very interesting environment for OE. This combination enables the integration of enhanced functionalities into usual textile materials, e.g. home textiles. Currently, there are mainly two different concepts about the integration of electronics in textiles called (i) in-cloth applications and (ii) on-cloth applications. In in-cloth applications, active devices such as OTFTs [5], [6], organic photovoltaics [7] and organic light emitting diodes [8] are implemented in the fibers and woven together to accomplish a electronic textile (e-textile). While on-cloth applications focus e.g. on producing thermal evaporated conductors with carbon nanotubes [9] or other polymers [10] or active devices such as sensors [11], batteries [12] and OTFTs [13], that are fabricated directly onto the textiles. Furthermore, there are also approaches to implement conventional silicon based electronics at item level in the textile fabric. The integration takes place at the final stage of the production chain of the clothing industry [14].

However, the most convenient integration of OE in textiles would be during their production stage as a semi-finished product. This requires a high stability of the OE devices since several textile processes need to be applied to finish the product. Despite several reported OE applications in textile fabrics, there is a lack of investigation and research regarding the degradation of the devices, especially under processes usually used in textile industry to transfer a semi-finished product onto a finished product.

The final home-textile product is also later on during its life-time subjected to similar stresses and strains, e.g. when washing it. The stresses and strains may originate in cooling from high temperature processes, chemical treatments and physical deformation. This paper reports on the degradation of the electrical performance of all-inkjet-printed OTFTs with TIPS-pentacene as the active semiconductor layer. The 6,13-bis(triisopropylsilylethynyl) pentacene (TIPS-pentacene) is one of the most widely studied organic p-type semiconductors and represents a good candidate for developing OE devices due to its high electrical performance [2], [15] and solubility in several organic solvents [16], [17]. It has also good stability against oxygen and humidity [18] and allows to obtain large crystalline structures by inkjet printing resulting in high electron mobility [3]. For the degradation study, the printed OTFTs are encapsulated and submitted to the industrial textile processes calendering, dyeing, washing and stentering. In this way, this investigation verifies the application limits of this type of materials and devices for the textile industry.

2. Experimental

The printing of all layers was performed with a Dimatix Materials Printer 2831 (DMP2831, Fujifilm Dimatix). The printer was equipped with piezo-electric printheads having 16 nozzles each with a diameter of about 21.5 µm. The nominal drop volume of the ejected droplet of the printhead is 10 pL. A 125 µm thick polyethylene naphthalate (PEN) film was used as substrate for the manufacturing of the OTFTs (TEONEX® Q65FA, DuPont Teijin Films).This substrate includes a pre-treatment on one side for improved adhesion, enabling the fabrication of high quality inkjet-printed patterns. According to the datasheet and further literature sources, it provides also good heat stability with a thermal shrinkage of only 0.4 % when exposed to 150 ºC for 30 minutes [19][20].

The OTFTs used in this contribution were manufactured in the bottom-gate bottom-contact (BGBC) architecture. With the BGBC geometry, the semiconductor is the last deposited layer in the multilayer structure and can be more affected by the different treatments for the degradation study. For the active layer, 1 wt % of 6,13-bis(triisopropylsilylethynyl) pentacene (TIPS-pentacene) (Sigma-Aldrich)

dissolved in 1,2-dichlorobenzene was inkjet-printed with a print resolution of 1270 dpi (corresponds to a center-to-center drop distance of 20 µm) and patterned as rectangle with a size of 3×1.25 mm^2. During printing, the substrate was heated to a temperature of 50 ºC to improve the layer formation. After the deposition of TIPS-pentance, the OTFTs were heated on a hotplate for 60 minutes at 50 ºC for final solvent evaporation and enhanced crystallization. The used temperature is in line with previous thermal treatment results that reported a temperature range between 46 ºC [21] and 60 ºC [22] to (i) avoid crack formation and to (ii) obtain enhanced crystallinity of the TIPS-pentacene film for high mobility. It has been shown [18] that the electrical characteristics of vapor-deposited TIPS-pentacene without any encapsulation degrade about ~ 30 % after 4 weeks exposure to ambient conditions. Moreover, it is reported that shorter channel length devices undergo significant degradation in threshold voltage [18] and on-current [18] with bias-stress [23]. However, the degradation of mobility and on/off ratio becomes less pronounced when heating of the devices is performed at temperatures close to 60 ºC. In this case, crack formation is reduced limiting the trapping sites for moisture or oxygen [22].

The silver (Ag) nanoparticle ink EMD5603 (SunChemical) was applied for the formation of the gate and source/drain electrodes. For the gate dielectric layer, the UV curable and commercially available ink formulation Hyperion Pro Wet Black (Tritron GmbH, Battenberg-Dodenau, Germany) was used. The thickness of the inkjet-printed silver layers are in the range of 400 to 500 nm. Since the UV curable ink formulation has no solvent components, the thickness of the dielectric is much higher (about 6 µm) compared to the silver layer. Several all-inkjet-printed OTFTs where manufactured with a channel width over length (W/L) ratio of 68200/10 µm and 61600/15 µm. Detailed information about the manufacturing process of the all-inkjet-printed OTFTs has been reported in [4].

Before the degradation study, a simple encapsulation of the printed OTFTs was done using the 125 µm thick PEN Teonex® Q65FA, similar to the one used as substrate, as top cover and ester polyurethane as adhesive. The PEN material was selected due to its effectiveness as a barrier against oxygen and moisture [24]. Ester polyurethane is a well-known elastomeric adhesive for different application, e.g. textiles, with high bond strength and wash resistance [25]. A scheme of the encapsulation barrier coating is shown in Fig. 1. The bonding was performed in a flat press maintaining the temperature at 115 ºC,

with a pressure of 30 N/cm^2 for 30 s. Temperature and pressure were applied only to the area defined by the ester polyurethane material to avoid the influence on the OTFT (see Fig. 1).

The encapsulated OTFTs were submitted to the industrial home-textile processes calendering, dyeing, washing and stentering within three weeks. The elapsed time between the device manufacturing including encapsulation and electrical performance measurement of the treated OTFTs was four weeks. Several OTFTs were subjected just to one process while others were submitted sequentially to all processes, following the natural industrial fabrication of the textile items.

Tab. 1 shows an overview of the different treatment processes, the process duration and the process conditions.

In the stentering process, the semi-finished textile substrates pass through a series of oven chambers for drying and/or heating of the textiles. Temperatures up to 130 °C and a low pressure due to the transport rollers were applied to the encapsulated OTFTs. The temperature treatments take about 200 s. Therefore, the stentering process was selected to study the influence of temperature on the electrical performance of the OTFTs.

In calendering, the OTFTs are subjected to high pressures as the textile passes through rollers where the applied pressure and the surface temperature can be regulated. Accordingly, the calendering process was chosen to study the influence of mechanical pressure on the electrical performance of the OTFTs.

In the dyeing process, the substrates are introduced into a solution with various dyes and auxiliary products dispersed in a medium for coloring. As a result, the dye process is appropriate to study the influence of the textile chemicals on the electrical performance of the encapsulated OTFTs. Finally, the washing process consists on passing the fabric through several tanks with a set temperature. Due to the nature of the textile industrial washing process, the OTFTs are subjected to a mechanical bending routine imposed by the transit of the fabric through cylinders to immerse the fabric in tanks containing soap and other chemicals for pH equalizing. The washing process used in this work has 50 cylinders with a

diameter of 13 cm where the fabric is immersed 24 times in the 4 tanks. All the industrial home-textile processes referred in this work subject the printed OTFTs to inwards and outwards bending processes at different points during the cycle. Based on all textile processes, namely stentering, calendering, dyeing, and washing, a study on the influence of temperature, pressure, exposure to chemicals and bending on the electrical performance of the encapsulated, all-inkjet-printed OTFTs is provided.

The optical images were obtained by a DM4000 (Leica Microsystems GmbH, Wetzlar, Germany) microscope. The electrical properties of the OTFTs were characterized by measuring the current–voltage (I–V) curves with a 2400 source/meter unit and a 6457 picoammeter with integrated voltage source from Keithley (Keithley Instruments, Cleveland, OH, USA). Both device fabrication and all measurements were performed in ambient conditions.

3. Results and Discussion

Fig. 2 shows the top view of an all-inkjet-printed OTFT consisting of a multilayer stack of gate electrode, dielectric, source/drain electrodes. The semiconductor layer is not shown here to ensure better visibility of the interdigitated source/drain electrodes. As it can be seen, the source/drain electrodes are well defined having comparable high edge sharpness and thus allowing the formation of a dense interdigitated network with a high channel width. The channel length has been optimized down to 10 µm using the laboratory inkjet printing system DMP2831.

Fig. 3a and 3b show the transfer and output characteristics, respectively, of the all-inkjet-printed OTFTs with the W/L ratio of 68200 µm/10 µm. The parameters were extracted short time after manufacturing without encapsulation and treatment. The obtained average values of the field effect mobility, on/off ratio, threshold voltage and subthreshold swing were 0.198 $cm^2\ V^{-1}\ s^{-1}$, 8×10^3, 3.15 V, and 3.2 V/dec. Fig. 3c and 3d show the transfer and output characteristics of the OTFTs with the W/L ratio of 61600 µm/15 µm. The average values of field effect mobility, on/off ratio, threshold voltage and subthreshold swing are 0.076 $cm^2\ V^{-1}\ s^{-1}$, 1.4×10^5, 4.05 V, and 2.2 V/dec, respectively.

Fig. 4 shows the overlap capacitance between the gate and S/D electrodes for the all-inkjet-printed OTFTs with the W/L ratio of 68200 µm/10 µm and 61600 µm/15 µm, before and after passing sequentially though all textile processes. The overlap capacitance was obtained in depletion mode. In the depletion mode, the overlap capacitance can be modeled as the series sum of two dielectrics, gate dielectric layer and depleted layer of pentacene. It is observed an increase of the OTFTs overlap capacitance after passing all textile processes when compared with the initial overlap capacitance. Due to the semiconductor layer being more exposed, the results suggests that a change in the depleted pentacene layer occurres mainly driven by the submission to the textile processes.Fig. 5 shows the transfer and output curves of the OTFTs with a W/L ratio of 68200 µm/10 µm (Fig. 5(a) and 5(b)) and corresponding curves for devices with W/L ratio of 61600 µm/15 µm (Fig. 5(c) and 5(d)), after passing through the different treatments of the textile manufacturing process (each graph is an average of data from three OTFTs). Both individual treatment processes as well as the sequence of all treatment processes are considered and compared with the OTFTs performance without any treatment (initial characterization). As can be observed the OTFTs maintain their basic electrical functionality in all cases. The treatment processes did not destroy the OTFTs, e.g. by short circuits due to a defective dielectric and similar reasons. However, there is a noticeable degradation of the electrical characteristics which depends on the textile process and the W/L ratio. The degradation seems to be more prominent for a W/L ratio of 68200 µm/10 µm as compared to 61600 µm/15 µm. Furthermore, the highest degradation is observed as expected when subjecting the OTFTs to all processes in a sequence.

The average values of field effect mobility, threshold voltage, on/off ratio, and subthreshold slope of the devices after passing through the different textile processes are shown in detail in Fig. 6(a)-(d).

3.1.Field effect mobility

The mobility of the OTFTs with L=15 µm is 60 % to 70 % less compared with the mobility of the device with L=10 µm. This is caused by an increased number of interface boundaries of the pentacene crystal with an increment of 50% in the channel length.

Fig. 6(a) shows the obtained field effect mobility of the OTFTs devices after submission to the different textile processes for both W/L ratios. The observed average degradation in the field effect mobility of the OTFTs with L=10 μm is about 34 % while for the L=15 μm the degradation is 23% when considering the treatment with all textile processes. The process with the largest influence on the field effect mobility was washing, followed by stentering. On the other hand, the process with the lowest influence was calendering, followed by dyeing. These results suggest that the bending at a regulated temperature of 98 ºC, introduced by the small diameter rolls during the washing process strongly decreased the obtained field effect mobility of the OTFTs. Previous works [13] have shown that the performance of the pentacene semiconductor does not vary after 30000 bending tests with OTFTs having a W/L ratio of 500 μm/25 μm. However, here much larger OTFTs were used and thus the impact of the bending is assumed to be higher. Additionally, the temperature application in the washing process has to be taken into account. It is expected thus that with the use of smaller OTFT structures, the influence of the bending present in washing will be less relevant.

The temperature of the stentering process appears as the second most influential physical condition on the field effect mobility. As shown in Fig. 6(a), the mobility decreased from 0.198 cm^2/V.s to 0.143 cm^2/V.s (about 28 %) for the OTFTs with L=10 μm and from 0.076 cm^2/V.s to 0.064 cm^2/V.s (about 16 %) for OTFTs with L=15 μm comparing the initial measurement and the measurement after the stentering process. According to a study related to the appearance of cracks in TIPS-pentacene films by exposure to temperature and mechanical forces [26], a phase transition takes place at 124 ºC which results in the development of cracks in the pentacene crystal film. In this study, tests were performed before and after heating the TIPS-pentacene. A decrease in field effect mobility between 50 % and 80 % was observed after heating to a temperature of 120 ºC for 20 minutes. Fig. 7 shows the optical microscope image of the pentacene crystal after sequential submission to all treatment processes. It is possible to observe the presence of interface regions in the pentacene crystal mainly with a direction perpendicular to the textile fabric process flow. Accordingly, the results obtained reflect the creation of the interface regions in the pentacene crystal by the effect of high temperature and by the bending

process, with the process of stentering being one of the most relevant due to the high temperatures that are close to the transition temperature of TIPS-pentacene.

The average degradation of the field effect mobility when subjecting the OTFTs to the dyeing process is about 20 % for the OTFTs with L=10 μm and 11 % for OTFTs with L=15 μm. The degradation observed after this process is lower than those observed in the processes of washing and stentering. As a result, moisture and chemicals have less influence on the degradation since the encapsulation of the OTFTs protects the semiconducting layer sufficiently, featuring temperature and bending as the parameters with more relevance.

Finally, the results show that the pressure applied in the calendering process has the lowest influence on the field effect mobility. The average degradation is 15 % for OTFTs with L=10 μm and 9 % for OTFTs with L=15 μm.

3.2. Threshold voltage

Fig. 6(b) shows the measured values of the threshold voltage. The results indicate that the threshold voltage undergoes a change of larger magnitude when the channel length is shorter (L=10 μm). A positive shift in the threshold voltage of 7.20 V appears in the OTFTs that are submitted sequentially to all treatment processes. In comparison, in the case of OTFTs with larger channel length (L=15 μm) the threshold voltage is positively shifted by 4.37 V. This implies an increase of the threshold voltage of 228 % for OTFTs with L=10 μm and 108 % for OTFTs with L= 15 μm. Therefore, the influence on lower channel length devices is again much higher than on larger channel length devices as already noticed for the field effect mobility.

Analogously to the degradation of field effect mobility, the threshold voltage is more influenced by the washing process, indicating that the mechanical effect of bending at a temperature of 98 ºC induces defects in the semiconductor. The second most influential physical-chemical condition on the threshold

voltage is the action of temperature through the stentering process, with an average increase of 4.06 V and 3.49 V (corresponds to an increase of 129 % and 86 %) for the different channel L=10 µm and L=15 µm, respectively. Finally, pressure, humidity and chemicals present in calendering and dyeing appear as physical-chemical conditions with less influence on the threshold voltage. This confirms the result of field effect mobility and indicates again the high stability of the encapsulation against humidity, pressure and various chemicals.

3.3. On/off current ratio

Fig. 6(c) shows the obtained on/off current ratio as a function of the different treatment processes of textile manufacturing for OTFTs with L=10 µm and L=15 µm. As for the other electrical parameters studied before, a degradation of the on/off current ratio is noticed when the OTFTs are submitted to the different treatment processes. The highest degradation of 66 % for OTFTs with L=10 µm and 40 % for OTFTs with L=15 µm was determined when exposing the samples to all treatment processes. Furthermore, the on-current I_{DS} is decreased to 13 % and 31 % while the off-current is increased up to 151 % and 25 % for the W/L=68200 µm/10 µm and W/L=61600 µm/15 µm channel OTFTs, respectively. Thus, the attenuation of the on/off current ratio is mainly due to the off-current fluctuation. As a result, the on/off current ratio undergoes a significant decrease when the channel length is shorter (L=10 µm) as compared to the larger channel length OTFTs (L=15 µm).

In accordance with the previous results, the on/off current ratio is more influenced by the bending mainly applied in the washing process. The temperature in the stentering process appears as a physical condition which induces a reduction in the on/off current ratio similar to bending. The effect of dyeing and calendaring on the threshold voltage is comparatively low.

3.4. Subthreshold slope

Figure 6(d) shows the average values of the subthreshold slope of the OTFTs. An increase of 0.6 V/dec is obtained for the OTFTs with L=10 µm and 0.85 V/dec for the OTFTs with L=15 µm.

Once again, the mechanical bending applied in the washing process has the biggest influence on the subthreshold slope with an increase 0.56 V/dec and 0.70 V/dec (corresponds to 18 % and 32 %). Calendering and dyeing have the lowest effect on the subthreshold slope.

4. Summary and conclusions

OTFTs with different W/L ratios were manufactured on flexible PEN substrate using inkjet printing. TIPS-pentacene was employed as semiconducting material. We could obtain a very low channel length in the range of 10 µm and 15 µm – without any pre-patterning or sophisticated alignment methods. The best OTFTs have an average field effect mobility of 0.198 $cm^2\ V^{-1}\ s^{-1}$ and an on/off ratio of about 1.4×10^5. After a simple encapsulation of the OTFTs, a degradation study was performed based on processes usually applied in textile manufacturing. The focus parameters were the field effect mobility, threshold voltage, on/off ratio and the subthreshold slope.

All the OTFTs were still functional after the different treatments. The influence of the physical treatments on the electrical performance are much more dominant than the chemical and temperature treatments. This implies that the encapsulation is very stable ensuring a good protection against water and oxygen over the time scale studied here [27]. However, since it is flexible and thin, it has limited protective properties against bending and temperature, respectively. Furthermore, we could identify a degradation of the electrical performance as a function of the treatment process and the W/L ratio. In all of our studies, a higher degradation occurred in the OTFTs with a shorter channel length (L=10 µm). We ascribe this result to defects in the crystal structure of TIPS-pentacene, which has more influence on the optimized performance of lower channel length OTFTs with the appearance of crystal interface regions characterized by poor mobility. The highest degradation obtained was for the on/off current. Here, the degradation was about 60 % followed by a positive shift in the threshold voltage of 7.20 V.

The mechanical bending introduced by the washing process is the condition that mainly influences the performance of the all-inkjet-printed OTFTs. Crack formation takes place in the semiconductor layer decreasing the electrical performance. However, it is expected that the electrical performance degradation caused by bending is minimized by the use of smaller OTFTs. Temperature is the physical

condition with the second largest influence on the printed OTFTs. The used encapsulation is relatively thin and the TIPS-pentacene film, after several minutes of exposure to high temperatures, initiate a phase transition inducing crack formation in the OTFTs.

The results obtained are encouraging for applications of OTFTs with TIPS-pentacene semiconductor integrated in textiles. Ensuring a proper encapsulation of the devices with our simple approach results in very high stability against water, moisture and chemicals usually applied in textile manufacturing. By limiting mechanical bending and high temperatures, the OTFTs still have sufficient electrical performance for potential functional applications integrated in textiles.

Acknowledgements

This work was supported by FEDER through the COMPETE Program and by the Portuguese Foundation for Science and Technology (FCT) in the framework of the Strategic Project PEST-C/FIS/UI607/2014 and the project PTDC/CTM-NAN/121038/2010. Enrico Sowade was financially supported by the European Commission within the Framework FP7-ICT (grant agreement number 287682, project acronym TDK4PE). The authors also thank for the support by the project Matepro – Optimizing Materials and Processes", ref. NORTE-07-0124-FEDER-000037", co-funded by the "Programa Operacional Regional do Norte" (ON.2 – O Novo Norte), under the "Quadro de Referência Estratégico Nacional" (QREN), through the "Fundo Europeu de Desenvolvimento Regional" (FEDER). Hélder Castro thanks for the support of the FCT under the grant SFRH/BDE/33350/2008.

References

[1] P. Jakimovski, T. Riedel, A. Hadda, M. Beigl, Design of a printed organic RFID circuit with an integrated sensor for smart labels, Int. Multi-Conf. on Syst., Sygnals & Devices (2012) 1–6.

[2] S. H. Lee, M. H. Choi, S. H. Han, D. J. Choo, J. Jang, S. K. Kwon, High-performance thin-film transistor with 6,13-bis(triisopropylsilylethynyl) pentacene by inkjet printing, Org. Electron. 9 (5) (2008) 721–726.

[3] S. Chung, J. Jang, J. Cho, C. Lee, S.-K. Kwon, Y. Hong, All-Inkjet-Printed Organic Thin-Film Transistors with Silver Gate, Source/Drain Electrodes, Jpn. J. Appl. Phys. 50 (3) (2011) 03CB05.

[4] H. F. Castro, E. Sowade, J. G. Rocha, P. Alpuim, S. Lanceros-Méndez, R. R. Baumann, All-Inkjet-Printed Bottom-Gate Thin-Film Transistors Using UV Curable Dielectric for Well-Defined Source-Drain Electrodes, J. Electron. Mater. 43 (7) (2014) 2631–2636.

[5] J. B. Lee, V. Subramanian, Weave Patterned Organic Transistors on Fiber for E-Textiles, IEEE Trans. Electron Devices 52 (2) (2005) 269–275.

[6] M. Maccioni, E. Orgiu, P. Cosseddu, S. Locci, A. Bonfiglio, Towards the textile transistor: Assembly and characterization of an organic field effect transistor with a cylindrical geometry, Appl. Phys. Lett. 89 (14) (2006) 143515.

[7] B. O'Connor, K. P. Pipe, M. Shtein, Fiber based organic photovoltaic devices, Appl. Phys. Lett. 92 (19) (2008) 193306.

[8] B. O'Connor, K. H. An, Y. Zhao, K. P. Pipe, M. Shtein, Fiber Shaped Light Emitting Device, Adv. Mater. 19 (22) (2007) 3897–3900.

[9] S. Khumpuang, K. Miyake, T. Itoh, Characterization of a SWNT-reinforced conductive polymer and patterning technique for applications of electronic textile, Sensors Actuators A: Phys. 169 (2) (2011) 378–382.

[10] T. . Yamashita, K. Miyake, T. Itoh, Characterization of conductive polymer coated silicone elastomer contact structure for woven electronic textile, Symp. Des. Test, Integr. Packag. MEMS/MOEMS (2012) 132–135.

[11] D. Chen, S. Lei, Y. Chen, A single polyaniline nanofiber field effect transistor and its gas sensing mechanisms, Sensors 11 (7) (2011) 6509–6516.

[12] R. Bhattacharya, M. M. de Kok, J. Zhou, Rechargeable electronic textile battery, Appl. Phys. Lett. 95 (22) (2009) 223305.

[13] G. S. Ryu, S. H. Jeong, B. C. Park, B. Park, C. K. Song, Fabrication of organic thin film transistors on Polyethylene Terephthalate (PET) fabric substrates, Org. Electron. 15 (7) (2014) 1672–1677.

[14] E. Legnani, S. Cavalieri, R. Pinto, S. Dotti, The Potential of RFID Technology in the Textile and Clothing Industry: Opportunities, Requirements and Challenges, in: D. C. C. Ranasinghe, Q. Z. Z. Sheng, S. Zeadally (Eds.), Unique Radio Innovation for the 21st Century, Springer Berlin Heidelberg, 2010, pp. 309–329.

[15] S. K. Park, T. N. Jackson, J. E. Anthony, D. A. Mourey, High mobility solution processed 6,13-bis(triisopropyl-silylethynyl) pentacene organic thin film transistors, Appl. Phys. Lett. 91 (6) (2007) 063514.

[16] W. H. Lee, D. H. Kim, Y. Jang, J. H. Cho, M. Hwang, Y. D. Park, Y. H. Kim, J. I. Han, K. Cho, Solution-processable pentacene microcrystal arrays for high performance organic field-effect transistors, Appl. Phys. Lett. 90 (13) (2007) 132106.

[17] C. S. Kim, S. Lee, E. D. Gomez, J. E. Anthony, Y.-L. Loo, Solvent-dependent electrical characteristics and stability of organic thin-film transistors with drop cast bis(triisopropylsilylethynyl) pentacene, Appl. Phys. Lett. 93 (10) (2008) 103302.

[18] S. K. Park, D. A. Mourey, J.-I. Han, J. E. Anthony, T. N. Jackson, Environmental and operational stability of solution-processed 6,13-bis(triisopropyl-silylethynyl) pentacene thin film transistors, Org. Electron. 10 (3) (2009) 486–490.

[19] W. S. Wong, A. Salleo (Eds.), Flexible Electronics: Materials and Applications, Springer, 2009.

[20] DuPont Teijin Films Teonex® PEN Film for Flexible Displays and Electronics, DuPont, 2011. Available: http://www2.dupont.com/Displays/en_US/products_services/films/PEN_film.html.

[21] M. W. Lee, G. S. Ryu, Y. U. Lee, C. Pearson, M. C. Petty, C. K. Song, Control of droplet morphology for inkjet-printed TIPS-pentacene transistors, Microelectron. Eng. 95 (2012) 1–4.

[22] J.-H. Bae, J. Park, C.-M. Keum, W.-H. Kim, M.-H. Kim, S.-O. Kim, S. K. Kwon, S.-D. Lee, Thermal annealing effect on the crack development and the stability of 6,13-bis(triisopropylsilylethynyl)-pentacene field-effect transistors with a solution-processed polymer insulator, Org. Electron. 11 (5) (2010) 784–788.

[23] C. R. Kagan, A. Afzali, and T. O. Graham, Operational and environmental stability of pentacene thin-film transistors, Appl. Phys. Lett. 86 (19) (2005) 193505.

[24] W. A. MacDonald, M. K. Looney, D. MacKerron, R. Eveson, R. Adam, K. Hashimoto, K. Rakos, Latest advances in substrates for flexible electronics, J. Soc. Inf. Disp. 15 (12) (2007) 1075.

[25] E. Toner, 3410 Product Datasheet, Bemis, 2009. Available: http://www.bemisworldwide.com/assets/Documents/3410.pdf.

[26] J. Chen, C. K. Tee, J. Yang, C. Shaw, M. Shtein, J. Anthony, D. C. Martin, Thermal and mechanical cracking in bis(triisopropylsilylethnyl) pentacene thin films, J. Polym. Sci. Part B: Polym. Phys. 44 (24) (2006) 3631–3641.

[27] S. Majee, M. F. Cerqueira, D. Tondelier, B. Geffroy, Y. Bonnassieux, P. Alpuim, J. E. Bourée, The effect of argon plasma treatment on the permeation barrier properties of silicon nitride layers, *Surf. Coatings Technol.* 235 (20.13) 361–366.

Figures and Figure Captions

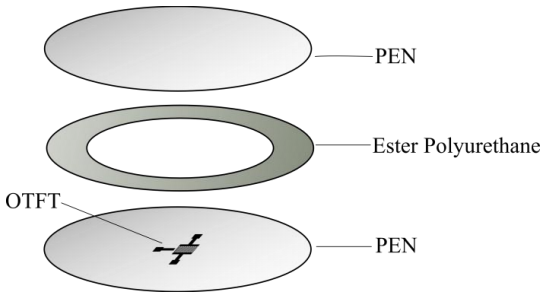

Fig. 1. Scheme of the encapsulation approach for the printed OTFTs.

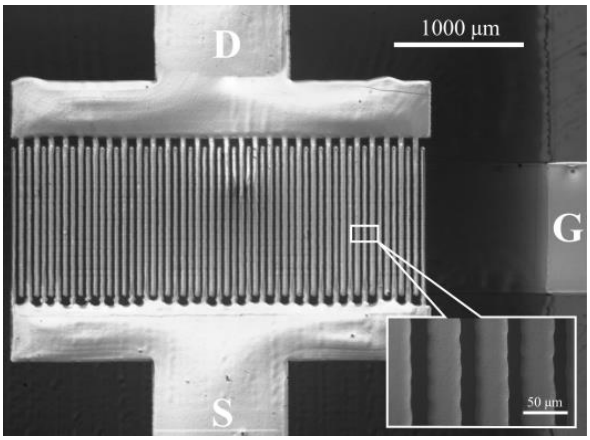

Fig. 2. Optical microscope image of the all-inkjet-printed OTFT structure with channel ratio W/L=61600/15 µm

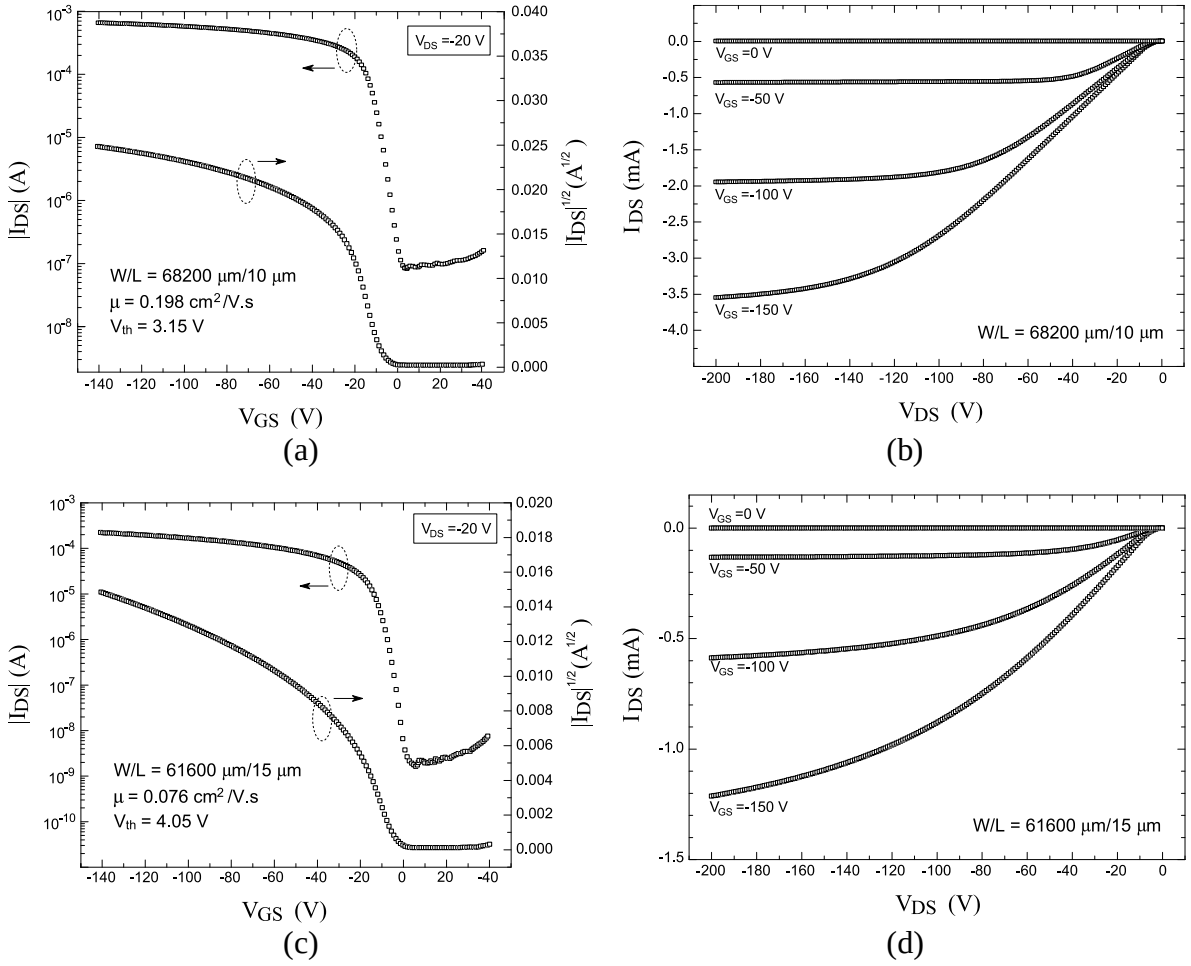

Fig. 3. Electrical characteristics of all-inkjet-printed OTFTs without any treatment. (a) Transfer and (b) output characteristics of the TFTs with W/L ratio of 68200 µm/10 µm. (c) Transfer and (d) output characteristics of the OTFTs with a W/L ratio of 61600 µm/15 µm.

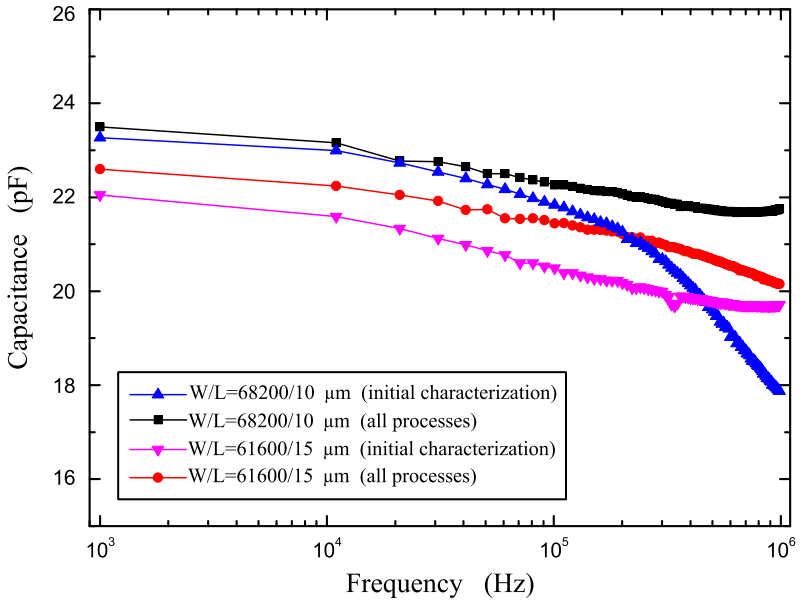

Fig. 4. Overlap capacitance as a function of frequency for the all-inkjet-printed OTFT with the channel ratio of W/L=68200 µm/10 µm and W/L=61600/15 µm.

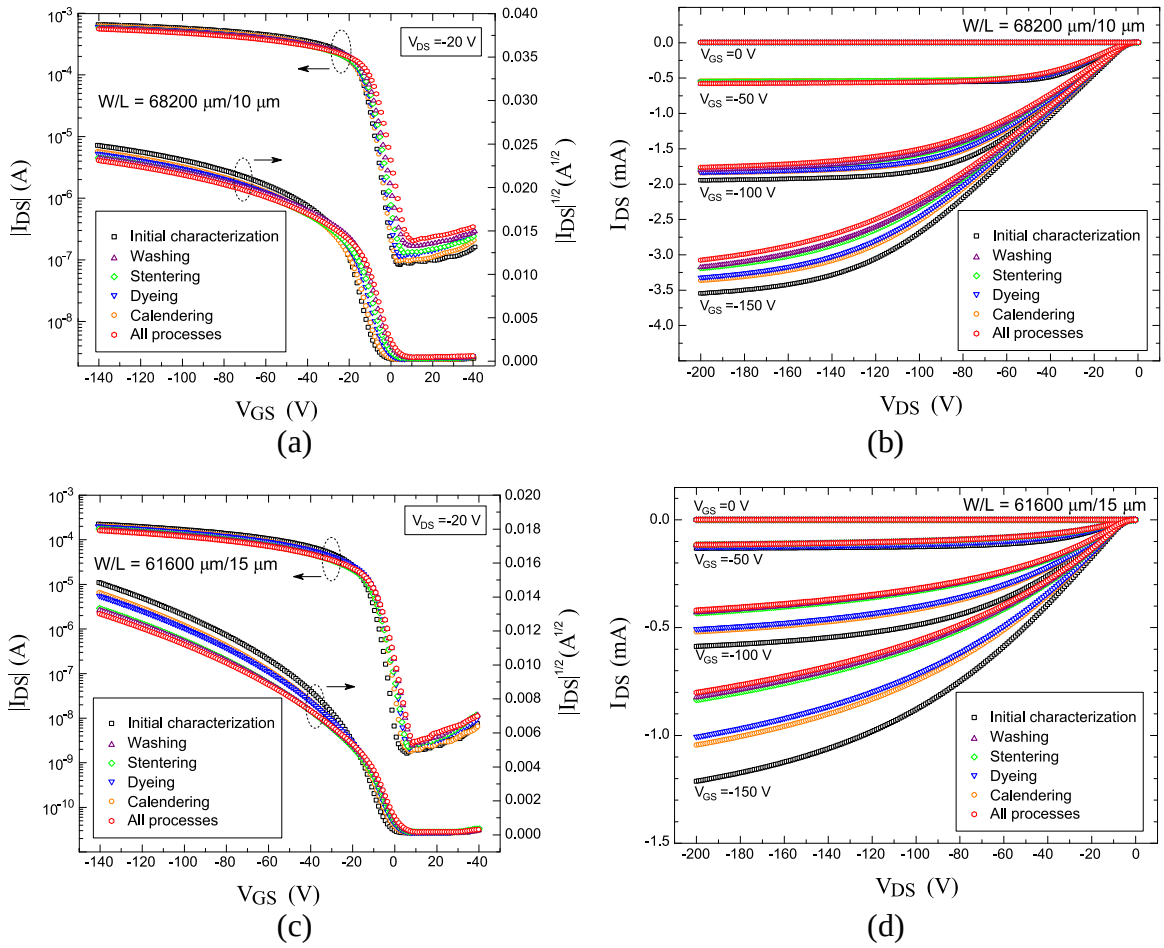

Fig. 5. Electrical characteristics of the printed OTFTs before and after submission to the different treatment processes applied in textile manufacturing. (a) Transfer and (b) output characteristics of OTFTs with W/L ratio of 68200 µm/10 µm (c) Transfer and (d) output characteristics of OTFTs with W/L ratio of 61600 µm/15 µm.

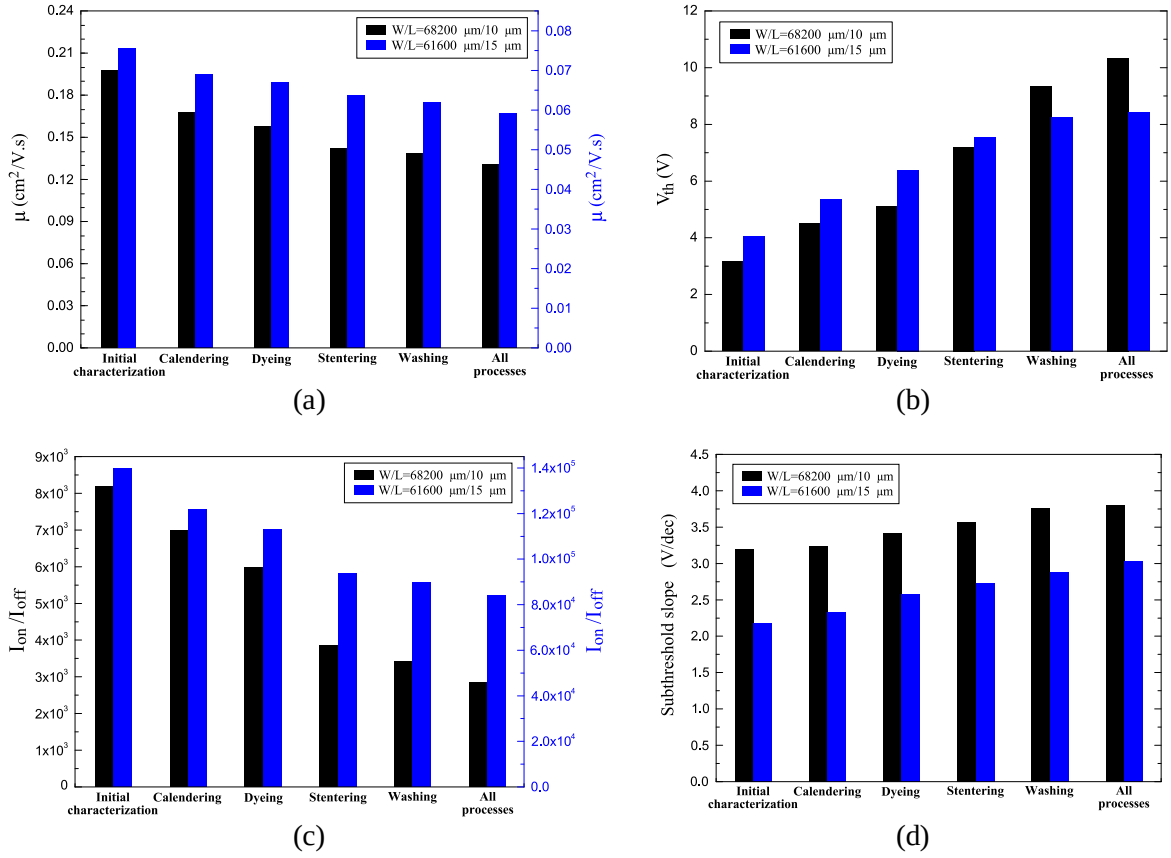

Fig. 6. Comparison of the (a) field effect mobility, (b) threshold voltage, (c) on/off ratio, and (d) subthreshold slope of the OTFTs with a W/L ratio of 68200 μm/10 μm and W/L ratio of 61600 μm /15 μm as a function of treatment process applied in textile manufacturing.

Tab. 1. Characteristics of the selected textile processes applied to the printed OTFTs.

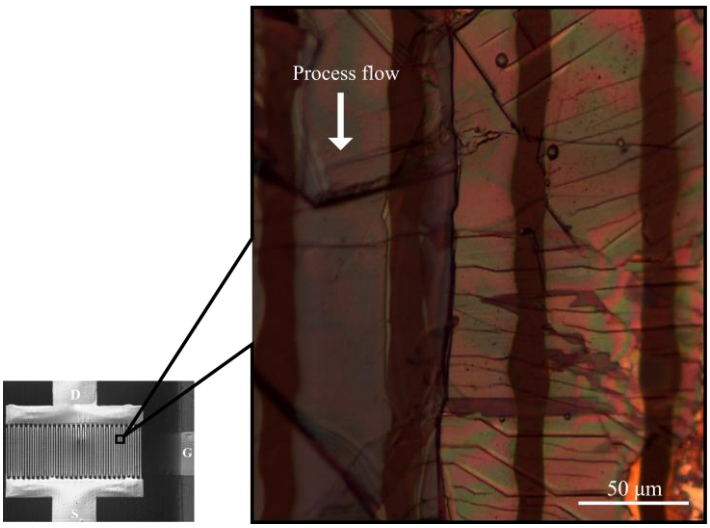

Fig. 7. Optical microscope image of the semiconductor in the OTFT after sequentially submitted to all home textile treatment processes.

Process	**Temperature [°C]**	**Pressure [N/cm^2]**	**Fabric Velocity [m/min]**	**Time of Process [s]**	**Number of passages**	**Chemicals**
Calender	98	305	25	20	1	---
Dye	98	---	70	1005	2	Sodium chloride; Dyes; Caustic soda; Sodium hydrosulfite; Hydrogen peroxide.
Wash	1st tank: 96 2nd tank: 96 3rd tank: 96 4th tank: 70	1.25	40	120	1	Soap; Acetic acid.
Stenter	1st chamber: 100 2nd chamber: 110 3rd chamber: 130 4th chamber: 130 5th chamber: 130 6th chamber: 130 7th chamber: 130 8th chamber: 130	0.87	15	200	1	---